

## K-BAND RED CLUMP DISTANCE TO THE LARGE MAGELLANIC CLOUD

DAVID R. ALVES,<sup>1</sup> MARINA REJKUBA,<sup>2,3</sup> DANTE MINNITI,<sup>3</sup> AND KEM H. COOK<sup>4</sup>

Received 2002 March 6; accepted 2002 May 24; published 2002 June 5

### ABSTRACT

The *Hipparcos* *I*-band calibration of horizontal-branch red clump giants as standard candles has lead to controversial results for the distance to the Large Magellanic Cloud (LMC). In an attempt to properly ascertain the corrections for interstellar extinction and clump age and metallicity, we analyze new multiwavelength luminosity functions of the LMC red clump. Our photometry data set in the *K* band was obtained with the Son of Isaac infrared imager at the European Southern Observatory's New Technology Telescope. In the *V* and *I* passbands, we employ data from the Wide Field Planetary Camera 2 on board the *Hubble Space Telescope*. The LMC red clump is first identified in a *K*, (*V*–*K*) color-magnitude diagram. Our luminosity functions yield apparent magnitudes of *K* = 16.974, *I* = 18.206, and *V* = 19.233 ( $\pm 0.009_r \pm 0.02_s$ ; random and systematic errors, respectively). Compared directly to the *Hipparcos* red clump calibration (without a correction for age and metallicity), the LMC clump measurements imply a negative interstellar reddening correction. This unphysical result indicates a population difference between clumps. A modified calibration based on theoretical modeling yields an average reddening correction of  $E(B-V) = 0.089 \pm 0.015$ , and a true LMC distance modulus of  $\mu_0 = 18.493 \pm 0.033_r \pm 0.03_s$ . We reconcile our result with the short distance previously derived from OGLE II red clump data.

**Subject headings:** distance scale — galaxies: distances and redshifts —  
 galaxies: individual (Large Magellanic Cloud) — Hertzsprung-Russell diagram —  
 stars: horizontal-branch

### 1. INTRODUCTION

The *Hipparcos* satellite mission yielded parallax measurements for hundreds of nearby red clump stars, and these are collectively the best-calibrated standard candle (Paczynski & Stanek 1998; Paczynski 2001). However, attempts to use the *Hipparcos* *I*-band red clump calibration to determine the distance to the Large Magellanic Cloud (LMC) have lead to controversial results. Udalski et al. (1998) obtained  $\mu_0 = 18.08 \pm 0.03_r \pm 0.12_s$  (random and systematic errors, respectively), which was subsequently revised upward to  $\mu_0 = 18.24 \pm 0.08$  (Udalski 2000). Stanek, Zaritsky, & Harris (1998) found  $\mu_0 = 18.07 \pm 0.03_r \pm 0.09_s$ . However, Zaritsky (1999) showed that the reddening correction used by Stanek et al. (1998) was overestimated. Romaniello et al. (2000) found  $\mu_0 = 18.59 \pm 0.04_r \pm 0.08_s$  by analyzing the *Hubble Space Telescope* (*HST*) photometry of the LMC red clump. Girardi & Salaris (2001) review these measurements and apply new model corrections for population effects (i.e., age and metallicity). They find a population correction in the *I* band of 0.2 mag. Consequently, they revise the Udalski (2000) result to  $\mu_0 = 18.37 \pm 0.07$  and the Zaritsky (1999) and Romaniello et al. (2000) result to  $\mu_0 = 18.55 \pm 0.05$ .

Alves (2000) demonstrated the use of the red clump as a standard candle at longer wavelengths; he calibrated the *Hipparcos* red clump absolute magnitude in the *K* band and applied the calibration to the Galactic bulge red clump. One advantage of working in this  $\sim 2 \mu\text{m}$  passband is the particularly small effect of extinction by interstellar dust (e.g., Schlegel, Finkbeiner, & Davis 1998). Grocholski & Sarajedini (2002) recently

studied population effects on the red clump's *K*-band absolute magnitude by compiling Two Micron All Sky Survey (2MASS) photometry of open clusters. They concluded that  $M_K$  is, in general, also less sensitive to population effects than  $M_I$ . The red clump models of Girardi & Salaris (2001) were also shown to be in fair agreement with the *K*-band open cluster data. In this Letter we present a deep *K*-band luminosity function for red clump stars in the LMC bar and inner disk. We also construct a *K*, (*V*–*K*) color-magnitude diagram (CMD) and complementary *V* and *I* luminosity functions. This is a first reconnaissance of optical and near-infrared photometry of the LMC red clump.

### 2. DATA

The six lines of sight studied in this Letter are centered on the source stars of LMC microlensing events discovered by the MACHO Project (events 4, 7, 9, 12, 14, and 18; Alcock et al. 2001). For our purposes, the lines of sight were selected at random by the natural occurrence of microlensing.<sup>5</sup> The six-field average line of sight intersects the LMC disk at  $\alpha = 05^{\text{h}}25^{\text{m}}55^{\text{s}}.2$ ,  $\delta = -70^{\circ}20'24''$  (J2000.0). This is  $0^{\circ}.49$  from the center of the LMC, nearly perpendicular to the line of nodes, and on the far side of the inclined disk (van der Marel et al. 2002). The geometric correction is small, about 0.6% in distance (0.013 mag), and in the sense that our clump giants are farther away than those at the LMC center.

The *K*-band data set analyzed here was obtained with the Son of Isaac (SOFI) infrared imager at the European Southern Observatory's New Technology Telescope; it is a  $1024 \times 1024$  array with a pixel size of  $0''.292$ . The total field of view of our trimmed (equal exposure) images after co-adding individual dithered frames is about  $140 \text{ arcmin}^2$ . The photometry was derived with DAOPHOT II (Stetson 1994) and calibrated with observations of six standard stars (Persson et al. 1998).

<sup>5</sup> Actually, event 12 may be a supernova in a galaxy behind the LMC, but this distinction does not affect the current work.

<sup>1</sup> Columbia Astrophysics Laboratory, Columbia University, 550 West 120th Street, New York, NY 10027; alves@astro.columbia.edu.

<sup>2</sup> European Southern Observatory, Karl-Schwarzschild-Strasse 2, D-85748 Garching, Germany; mrejkuba@eso.org.

<sup>3</sup> Departamento de Astronomía y Astrofísica, Pontificia Universidad Católica, Casilla 306, Santiago 22, Chile; dante@astro.puc.cl.

<sup>4</sup> Lawrence Livermore National Laboratory, 7000 East Avenue, Livermore, CA 94550; kcook@llnl.gov.

Conditions were photometric (Rejkuba et al. 2001). The  $1\sigma$  standard deviation of the calibration solution is 0.028 mag. Over 98% of the stars in the red clump (or brighter;  $K < 18$ ) were detected with a signal-to-noise ratio  $S/N > 10$ , and thus our SOFI red clump data are nearly complete. The  $K_s$  magnitude system employed (“ $K$  short”) is the same as 2MASS. In order to check our standardized zero point, we matched a subset of the SOFI data with 2MASS second incremental release photometry.<sup>6</sup> A comparison shows no zero-point difference to within 0.02 mag (for stars with colors like the red clump). However, all of the stars in the comparison are actually redder and brighter than the clump, and thus the agreement found lends only weak support to the accuracy of our data. Finally,  $K_s$  magnitudes are related to the  $K$ -band red clump data compiled by Alves (2000) by  $K = K_s + 0.044$  (Grocholski & Sarajedini 2002; their eq. [2]). We transform  $K_s$  to  $K$  accordingly.

Our data set in  $V$  and  $I$  was obtained with the Wide Field Planetary Camera 2 (WFPC2) on board *HST* (PI: K. H. Cook). We exclude the PC2 images from our analysis. This guarantees a homogeneous  $V$  and  $I$  photometry data set and represents only a small loss in imaged area. The three WF observations are  $800 \times 800$  pixel<sup>2</sup> arrays with a pixel size of  $0''.1$ . The resulting total field of view is approximately 32 arcmin<sup>2</sup>. The *HST*/WF instrumental F555W and F814W magnitudes were derived with DAOPHOT II and calibrated to Landolt’s  $V$  and  $I$  with an accuracy of 0.02–0.03 mag following the usual procedures (Alcock et al. 2001). Nearly all of the LMC clump giants were detected with a very high signal-to-noise ratio. In order to check our  $V$  and  $I$  zero points, we cross-correlated a subset of our data with OGLE II ground-based photometry<sup>7</sup> (Udalski et al. 2000). A comparison reveals zero-point differences of  $\Delta V = 0.11$  mag and  $\Delta I = 0.02$  mag in the sense that OGLE II is brighter. Alcock et al. (1999) compared MACHO ground-based photometry with an early reduction of these same standardized *HST*/WF data (a different subset) and found that MACHO was brighter by  $\Delta V = 0.06$  mag and  $\Delta R = 0.00$  mag. We speculate that the aperture corrections applied to the OGLE II and MACHO ground-based  $V$  data may be affected at the 5%–10% level by crowding errors. For example, it is possible that the  $V$ -band “sky” around bright stars used to determine the aperture corrections was on average underestimated because nearby neighbor stars were oversubtracted (Alcock et al. 1999; Udalski et al. 2000). We tentatively adopt a formal systematic calibration error of 0.02 mag in  $V$  and  $I$  based on the stated accuracy of *HST*/WF calibrations.

### 3. ANALYSIS AND RESULTS

We detected approximately 36,000 stars in  $K$  and 109,000 stars in  $V$  and  $I$ . Of these, approximately 27,000 have  $K < 20$  and 7000 have  $V < 21$ . Cross-correlating these latter source lists yields 4745 stars with  $K$ ,  $I$ , and  $V$  magnitudes. Figure 1 shows the resulting  $K$ ,  $(V-K)$  CMD in the region around the red clump. Only 2353 stars appear within the limits of Figure 1, and we restrict our subsequent analyses to these stars. As discussed by Alves (2000 and references therein), not all of the stars appearing in Figure 1 are bona fide red clump giants. The first-ascent red giant branch (RGB) is identified as the roughly vertical sequence running from  $(V-K) \sim 2.2$  at

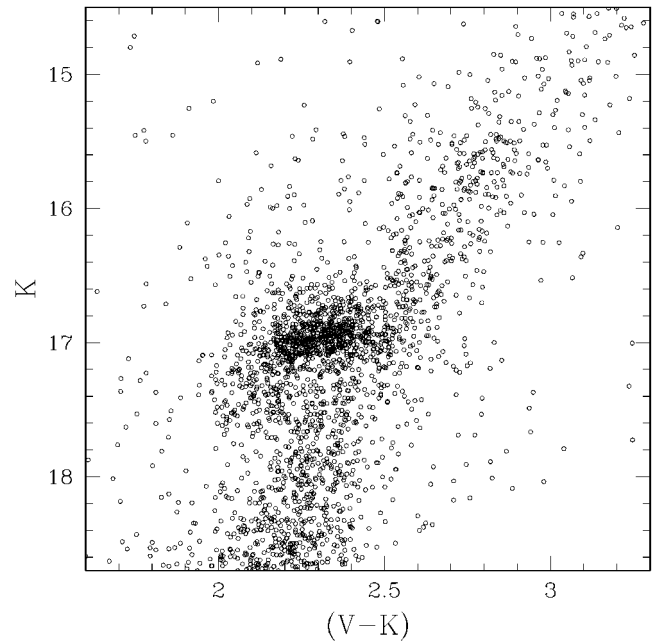


FIG. 1.— $K$ ,  $(V-K)$  CMD of the LMC red clump (2353 stars). The red clump appears at  $K \sim 17$  and lies mostly blueward of the giant branch. Error bars on the individual data points are about the size of the symbols plotted (*open circles*) at the brightness of the red clump.

$K \sim 18.5$  to  $(V-K) \sim 3.1$  at  $K \sim 14.5$ . It has a width of about 0.2 mag in  $(V-K)$  color, and no distinct component branches are evident. Some of these stars are second-ascent asymptotic giant branch (AGB) stars. The distinction between an RGB and AGB star is not necessarily clear in a CMD of mixed age field populations like this one. The sought-after horizontal-branch red clump is the most prominent feature in Figure 1. It appears at  $K \sim 17$  and lies mostly blueward of the giant branch, i.e.,  $(V-K) \lesssim 2.4$ . The detailed structure of the clump seen here is well understood in the context of stellar evolution theory (Girardi & Salaris 2001). The overdensity of stars with  $K \sim 17$  and colors that associate them with the giant branch (i.e.,  $V-K \sim 2.4$ – $2.5$ ) may be the first detection of the “RGB bump” for LMC field stars (see Fig. 19 of Girardi & Salaris 2001). The RGB bump is an evolutionary pause as the hydrogen-burning shell crosses a chemical composition discontinuity. The loose clustering of stars seen on the giant branch at  $(V-K) \sim 2.8$  and  $K \sim 15.5$  may be the “AGB bump,” an evolutionary pause at the onset of helium shell burning (see, e.g., Alves & Sarajedini 1999).

A side-by-side comparison of red clump luminosity functions (LFs) is presented in Figure 2. The LMC clump is shown on the left. The *Hipparcos* clump is shown on the right (data from Alves 2000). The LFs in  $K$ ,  $I$ , and  $V$  are each plotted in separate panels (*top to bottom*). LMC bin size is 0.05 mag; *Hipparcos* bin size is 0.10 mag; each panel is 1.5 mag wide. The adopted model LFs (Fig. 2, *solid lines*) are a superposition of a linear background and a Gaussian of variable width, amplitude, and location. The backgrounds are fitted in restricted magnitude ranges that exclude the clump. The best-fit model parameters and  $\chi^2$  (per degrees of freedom, or dof) are provided in Table 1. The LMC red clump in Figure 2 totals about 2000 stars. For comparison, there are 238 *Hipparcos* red clump stars with  $K$ ,  $I$ , and  $V$  data (Alves 2000). This distinction reflects in the formal statistical errors for the peak clump brightnesses given

<sup>6</sup> See <http://www.ipac.caltech.edu/2mass>.

<sup>7</sup> See <http://sirius.astrouw.edu.pl/ogle>.

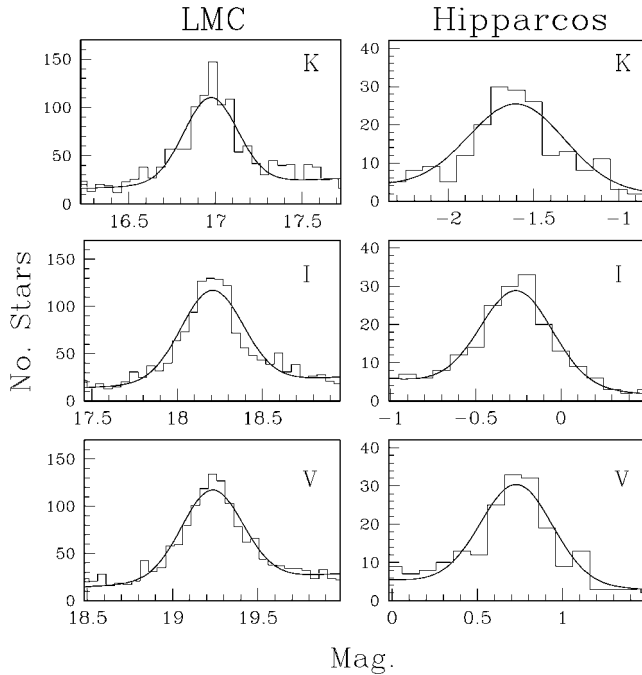


FIG. 2.— $K$ ,  $I$ , and  $V$  LFs for the LMC red clump are shown in the left panels (bin size 0.05 mag). In the right panels, the  $K$ ,  $I$ , and  $V$  LFs for the *Hipparcos* red clump are shown (bin size 0.1 mag). Best-fit model functions consisting of a Gaussian and a linear background are overplotted as solid lines. These model fits yield the peak brightness of the red clump in each passband.

in Table 1. Despite the shortcomings of our model LFs revealed in Figure 2, the peak brightnesses of the red clumps are evidently well determined.

The *Hipparcos* calibration assumes no reddening correction, as suggested by Stanek & Garnavich (1998). These authors argue that the average reddening is probably  $E(B-V) < 0.02$  mag. It should be kept in mind that the LMC distance derived in this work is practically independent of the reddening correction applied to the *Hipparcos* clump. However, the average LMC reddening obtained in comparison may be slightly underestimated. We note that the Lutz-Kelker correction to the Alves (2000) calibration data set is probably also negligible (Udalski 2000). The true LMC distance modulus is therefore given by

$$\mu_0 = (m-M)_0 = (m-M)_\lambda - A_\lambda + \Delta M_\lambda, \quad (1)$$

where  $\lambda$  corresponds to  $K$ ,  $I$ , or  $V$  and the apparent distance moduli in each passband are  $(m-M)_\lambda$ . The corrections for population effects are  $\Delta M_\lambda = M_\lambda(\text{Hipparcos}) - M_\lambda(\text{LMC})$ , following the convention of Girardi & Salaris (2001). These corrections, the inverse effective wavelengths of each passband ( $\mu\text{m}^{-1}$ ), and the adopted reddening law ( $A_\lambda$ ; Schlegel et al. 1998) are all summarized in Table 1. The results of this work are insensitive to small uncertainties in the reddening law or effective wavelengths employed. Although omitted from equation (1), we also apply a geometric correction to our final distance estimate (see below).

We first compare the LMC and *Hipparcos* red clumps by assuming  $\Delta M_\lambda = 0$ . The resulting apparent distance moduli are plotted as a function of inverse effective wavelength in Figure 3 (*open circles*; error bars omitted) and listed in Table 1. A fit for the average interstellar reddening and true LMC distance modulus yields  $E(B-V) = -0.026 \pm 0.014_r$  and

TABLE 1  
RED CLUMP DATA

Quantity	$K$	$I$	$V$
$\lambda^{-1} (\mu\text{m}^{-1})$ .....	0.48	1.24	1.81
$A_\lambda/E(B-V)^a$ .....	0.35	1.96	3.24
$m_\lambda^b$ .....	$16.974 \pm 0.009$	$18.206 \pm 0.009$	$19.233 \pm 0.009$
$\sigma_\lambda$ .....	0.155	0.182	0.180
$\chi^2$ .....	2.2	2.1	1.6
$M_\lambda^c$ .....	$-1.60 \pm 0.03$	$-0.26 \pm 0.03$	$0.73 \pm 0.03$
$\sigma_\lambda$ .....	0.28	0.21	0.21
$\chi^2$ .....	1.4	0.9	1.7
$(m-M)_\lambda$ .....	18.57	18.47	18.50
$\Delta M_\lambda^d$ .....	-0.03	0.20	0.30
$M_\lambda$ .....	$-1.57 \pm 0.03$	$-0.46 \pm 0.03$	$0.43 \pm 0.03$
$(m-M)_\lambda$ .....	$18.54 \pm 0.03$	$18.67 \pm 0.03$	$18.80 \pm 0.03$

<sup>a</sup> Adopted reddening law from Schlegel et al. 1998, which refers to the effective wavelength of each passband.

<sup>b</sup> Peak brightness and width of the LMC clump, followed by  $\chi^2/\text{dof}$  of the best-fit model LF.

<sup>c</sup> Peak brightness and width of the *Hipparcos* clump (data from Alves 2000), followed by  $\chi^2/\text{dof}$  of the best-fit model LF. The LMC apparent distance moduli based on this calibration are given on the next line (see text).

<sup>d</sup> The population correction for the LMC red clump absolute magnitude calculated from theoretical models (Girardi & Salaris 2001). The modified *Hipparcos* calibration is given on the next line, followed by the resulting LMC apparent distance moduli.

$(m-M)_0 = 18.562 \pm 0.033_r$ , which is shown as the dotted line in Figure 2. A negative reddening correction is unphysical and indicates a significant population difference between the LMC and *Hipparcos* red clumps. In order to account for the population difference, we appeal to the theoretical calculations of Girardi & Salaris (2001). These authors generated artificial LMC and *Hipparcos* red clumps from a grid of core helium-burning stellar

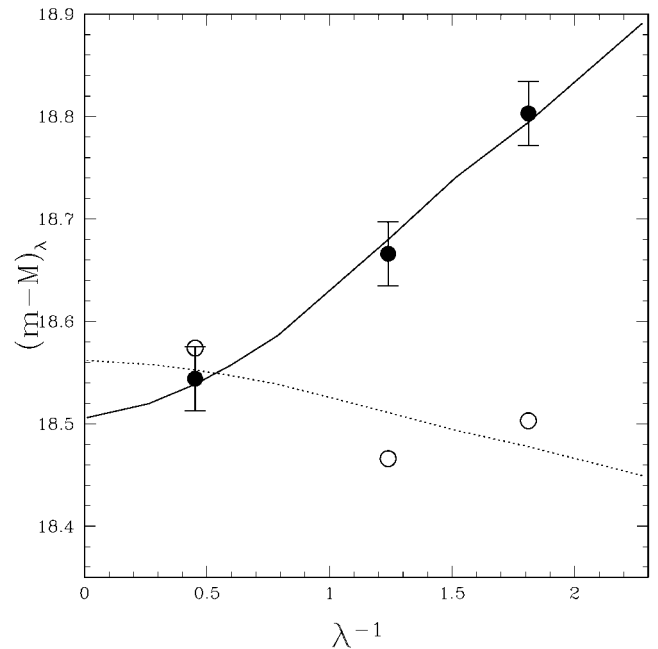


FIG. 3.—Apparent LMC distance moduli plotted as a function of inverse effective wavelength ( $\mu\text{m}^{-1}$ ). Open circles (error bars omitted) are based on the *Hipparcos* calibration without adjustment for population effects. Best fit for the mean interstellar reddening correction and true LMC distance modulus is shown as a dotted line. Filled circles (with error bars) are based on the *Hipparcos* calibration modified for a mean population difference in the LMC. Solid line through these data points shows the best-fit mean interstellar reddening correction and true LMC distance modulus:  $E(B-V) = 0.089 \pm 0.015_r$  and  $(m-M)_0 = 18.506 \pm 0.033_r$ .

models. Each clump refers to specific star formation and chemical enrichment histories reported in the literature and is thus constrained at least indirectly by observational data. Possible systematic errors associated with the zero points of the theoretical models would cancel in the first-order approximation because the population corrections are calculated only in a relative sense. This calculation predicts  $\Delta M_I = 0.20$  mag (§ 1). In a private communication (L. Girardi & M. Salaris 2002), the same artificial clumps yield population corrections of  $\Delta M_V = 0.30$  and  $\Delta M_K = -0.03$  (Table 1). The  $K$ -band absolute magnitude has the smallest correction, in agreement with the trend noted by Grocholski & Sarajedini (2002). The resulting modified apparent distance moduli are plotted in Figure 3 (*solid circles with error bars*) and listed in Table 1. Solving for the reddening and true distance modulus yields  $E(B-V) = 0.089 \pm 0.015_r$  and  $(m-M)_0 = 18.506 \pm 0.033_r$  (Fig. 3, *solid line*). The excellent fit of the red clump data in Figure 3 lends indirect support to the photometric zero points adopted in this work. Applying a small correction for the inclination of the LMC disk and the location of our fields (§ 2), the true LMC distance modulus is  $(m-M)_0 = 18.493 \pm 0.033_r$ .

#### 4. CONCLUSION

We have presented new multiwavelength LFs of LMC red clump stars. Our analysis yields a distance modulus of  $\mu_0 = 18.493 \pm 0.033_r$ . The  $K$ -band red clump distance to the LMC is  $49.96 \pm 0.77$  kpc in good agreement with the average published value (50.1 kpc; Freedman et al. 2001). We have also derived an average reddening of  $E(B-V) = 0.089 \pm 0.015_r$ . For comparison, the Galactic foreground reddening in this direction is  $E(B-V) = 0.06 \pm 0.02$  (Oestreich, Goehrmann, & Schmidt-Kaler 1995). Our mean reddening result is consistent with the foreground reddening, and this is a success of the Girardi & Salaris (2001) models.

The statistical error associated with our new distance result is due to the *Hipparcos* calibration (3%) and measuring the LMC red clump brightnesses (1%). The overall systematic error may be comparable. Our photometry is standardized with a 2% systematic uncertainty. This error is also uncorrelated between  $K$  and  $V$  or  $I$ . However, our zero-point checks do not support this level of photometric accuracy unless ground-based comparison data are in some cases too bright by up to 0.1 mag. We have

suggested that this may be possible. Uncertainties in our reddening and geometric corrections contribute negligible systematic error to the distance result. The systematic error due to the population correction is probably also small. The worst case of making no correction at all leads to a change in modulus of less than 6%. However, this also yields a negative reddening correction. For realistic reddenings, the population correction to the true distance modulus is approximately the same as the correction in the  $K$  band (3%). In summary, the systematic errors in our  $K$ -band red clump distance to the LMC are probably on the order of 2% (photometric calibration) and 3% (population correction) and are thus comparable to the statistical error obtained.

The  $K$ -band red clump distance to the LMC is in agreement with previously reported  $I$ -band results (§ 1). The only serious discrepancy is the short distance result of Udalski (2000) based on OGLE II data. Udalski (2000) finds a mean dereddened red clump brightness of  $I_0 = 17.944 \pm 0.014_r$  for nine fields in the LMC halo. Those fields are on average  $2.12^\circ$  from the center of the LMC, nearly perpendicular to the line of nodes and on the *near* side of the inclined disk (van der Marel et al. 2002). Correcting for the 0.02 mag zero-point offset between OGLE II and our *HST*/WF data, and for geometric projection, the Udalski (2000) red clump brightness becomes  $I_0 = 18.024$  mag (at LMC center). For comparison, our dereddened red clump brightness (Table 1) corrected to the LMC center is  $I_0 = 18.019$  mag. The results of this work, Udalski (2000), and Romaniello et al. (2000) therefore all agree, which lends strong support to the accuracy of the  $K$ -band red clump distance to the LMC.

D. R. A. acknowledges the referee, K. Z. Stanek, for his helpful comments, L. Girardi and M. Salaris for their communications, and A. Crotts for support (grant AST 00-70882). D. M. is supported by FONDAP Center for Astrophysics and FONDECYT. This Letter is based on observations made with the NASA/ESA *Hubble Space Telescope*, obtained at STScI, operated by AURA, Inc., under NASA contract NAS 5-26555 (GO proposal 5901 and 7306 to K. H. C.). This work was performed under the auspices of the US Department of Energy, National Nuclear Security Administration by UC-LLNL (contract W-7405-Eng-48). Use of 2MASS data, a joint project of the University of Massachusetts and IPAC/Caltech funded by NASA and the NSF, is acknowledged.

#### REFERENCES

- Alcock, C., et al. 1999, *PASP*, 111, 1539  
 ———. 2001, *ApJ*, 552, 582  
 Alves, D. R. 2000, *ApJ*, 539, 732  
 Alves, D. R., & Sarajedini, A. 1999, *ApJ*, 511, 225  
 Freedman, W., et al. 2001, *ApJ*, 553, 47  
 Girardi, L., & Salaris, M. 2001, *MNRAS*, 323, 109  
 Grocholski, A., & Sarajedini, A. 2002, *AJ*, 123, 1603  
 Oestreich, M. O., Goehrmann, J., & Schmidt-Kaler, T. 1995, *A&AS*, 112, 495  
 Paczyński, B. 2001, *Acta Astron.*, 51, 81  
 Paczyński, B., & Stanek, K. Z. 1998, *ApJ*, 494, L219  
 Persson, S. E., Murphy, D. C., Krzemiński, W., Roth, M., & Rieke, M. J. 1998, *AJ*, 116, 2475  
 Rejkuba, M., Minniti, D., Silva, D. R., & Bedding, T. 2001, *A&A*, 379, 781  
 Romaniello, M., Salaris, M., Cassis, S., & Panagia, N. 2000, *ApJ*, 530, 738  
 Schlegel, D. J., Finkbeiner, D. P., & Davis, M. 1998, *ApJ*, 500, 525  
 Stanek, K. Z., & Garnavich, P. M. 1998, *ApJ*, 503, L131  
 Stanek, K. Z., Zaritsky, D., & Harris, J. 1998, *ApJ*, 500, L141  
 Stetson, P. 1994, *PASP*, 106, 250  
 Udalski, A. 2000, *ApJ*, 531, L25  
 Udalski, A., Szymanski, M., Kubiak, M., Pietrzynski, G., Wozniak, P., & Zebrun, K. 1998, *Acta Astron.*, 48, 1  
 Udalski, A., et al. 2000, *Acta Astron.*, 50, 307  
 van der Marel, R., Alves, D. R., Hardy, E., & Suntzeff, N. 2002, preprint (astro-ph/0205161)  
 Zaritsky, D. 1999, *AJ*, 118, 2824